

# Design and Performance of 10 Gb/s Optical Receiver in 50-GHz DWDM Transmission over 40-km SSF

Duang-rudee Worasuchep<sup>1</sup>,

Wanee Srisuwarat<sup>2</sup>, and Jirawut Akaranuchat<sup>3</sup>, Non-members

## ABSTRACT

This paper describes the design of 10 Gb/s optical receiver, which consists of an Avalanche Photo-Detector (APD) and a Clock & Data Recovery (CDR) circuit. All components are successfully integrated onto the 4-layered FR-4 PCB, using two types of signal paths: differential microstrip and single-ended CB-CPW. Their dimensions are optimally chosen for matching impedance, according to the ADS simulations. The receiver's performance has been evaluated under 3 impairments: jitter, interchannel crosstalk and fiber dispersion. The Periodic Jitter (PJ) is added to analyze histograms and measure the receiver's jitter tolerance. The crosstalk and dispersion effects on eye-diagram are demonstrated via the testbed of 50-GHz Dense Wavelength Division Multiplexing (DWDM) transmission over 40-km Standard Single Mode Fiber (SSMF). The measured jitter tolerance proves that this receiver can pass the SONET (Synchronous Optical Network) mask standard with Bit Error Rate (BER) below  $10^{-12}$ . The recovered eye-diagrams show that this design can reduce both crosstalk and dispersion effects. The power penalty of this receiver is determined from the BER plot to be within 2-dB standard limit.

**Keywords:** Optical Receiver, Jitter, Crosstalk. Dispersion

## 1. INTRODUCTION

Optical fiber communication has become popular due to its tremendous bandwidth and low attenuation. The main focus of research and development is to increase data rate of all components inside both optical transmitter and optical receiver up to multi Gb/s range. The current bit rate per channel is 40 Gb/s for chipset [1] and optical modulator [2]. Meanwhile, the performance criteria of high-speed data transmission are constantly better. For example, a

typical  $10^{-9}$  BER is replaced by  $10^{-12}$  BER or error-free transmission. Moreover, the jitter impairment deteriorates as data rate increases. The jitter generation of optical transmitter as well as the jitter tolerance of optical receiver must be exceptional; otherwise, the BER will be worse. In order to sustain such strict criteria, some additional circuits are required, such as, an equalizer and CDR circuit with integrated low-noise amplifier.

The total transmission capacity of WDM system is upgradable either by increasing a number of channels or decreasing a channel space between adjacent channels. To lower a system's cost, the Coarse WDM (CWDM) is generally chosen with fixed 20 nm channel spacing. In contrast, the DWDM system has many channel spacings: 200, 100, 50, 25 and 12.5 GHz (equivalent to 1.6, 0.8, 0.4, 0.2 and 0.1 nm at  $\sim 1550$  nm wavelength) according to the ITU-T G.694.1 standard of spectral grids for WDM application. This tight spacing requires expensive lasers with more stable and narrower spectral widths. Multiple optical transmitters and receivers can be integrated into one WDM transceiver, for instance, 4 channel  $\times$  10 Gb/s transceiver for CWDM [3] and DWDM [4] at 200 GHz spacing. Most DWDM systems use 100 GHz spacing [5]. The 50 and 25 GHz [6] spacings are preferred for higher capacity, however, with additional power penalty due to a severe channel crosstalk.

DWDM system is usually installed as core networks with a standard transmission distance of 2, 15, 40, 80, 120 or 160 km. This distance is another performance criterion. Two impairments occur when using a long SSF: fiber attenuation and Group Velocity Dispersion (GVD). First, the attenuation can be compensated by optical amplifiers, such as Erbium Doped Fiber Amplifier (EDFA). Second, the GVD, which causes pulse spreading, can be mended by using Dispersion Compensation Fiber (DCF) that has a large negative dispersion. For the 10 Gb/s system over 40 km long SSF at 1550-nm wavelength, both EDFA and DCF are deployed according to the ITU-T G.691 standard [7]; however, they raise the total cost of system.

In this work, the design of 10 Gb/s optical receiver is described. It consists of an APD, a CDR circuit and a 155 MHz reference clock soldered on a

Manuscript received on July 28, 2010 ; revised on November 24, 2010.

This paper is extended from the paper presented in ECTI-CON 2010.

<sup>1,2,3</sup> The authors are with Electrical Engineering Department, Chulalongkorn University, Bangkok, Thailand, E-mail: duangrudee.w@chula.ac.th, return\_19@hotmail.com and officia@hotmail.com

4-layered Printed Circuit Board (PCB). The aim of this paper is to demonstrate a successful integration of those commercially available components onto a commonly manufactured FR-4 PCB, not a specially required highperformance dielectric. Using the licensed Advanced Design System (ADS) software and other free ware, the routes and dimensions of signal paths between every pair of components were simulated for matching impedance and optimally chosen under some realistic constraints, such as the limitations of PCB fabrication, the smallest PCB, a minimal number of design cycles, and the lowest cost per prototype. Different PCB designs were simulated, but only the best two versions were selected for fabrication. This optical receiver was assembled as our first prototype and it can pass all the following tests.

The receivers performance has been evaluated under three impairments: jitter, interchannel crosstalk and GVD. To analyze jitter, the PJ is injected into PG to measure jitter histograms and the jitter tolerance of receiver. The resulted jitter tolerance shows that this receiver can pass the SONET mask standard with BER below  $10^{-12}$  across the jitter frequency range between 0.7 and 80 MHz. Subsequently, to analyze crosstalk and GVD, three 50- GHz DWDM channels are transmitted over 40 km long SSMF and the received 10 Gb/s eye-diagrams are measured. This transmission condition is properly chosen from those described standards and in agreement with a specification of 10 Gb/s optical transmitters used in the experimental testbed. Since the receiver can reduce both crosstalk and dispersion effects via its CDR circuit, the recovered eye-diagrams can successfully pass the STM-64/OC-192 data mask standard. The BER performance of this receiver is also measured showing the power penalty at  $10^{-9}$  BER within 2-dB standard limit.

The remainder of this paper is organized as follows. Section 2 explains about jitter, interchannel crosstalk and GVD. Section 3 describes the design and components of 10 Gb/s optical receiver. Section 4 shows block diagrams of three measurement setups: jitter histogram, jitter tolerance, and DWDM transmission testbed. Section 5 analyzes the results, including jitter histograms, jitter tolerance, eye-diagrams and BER plot. Finally, section 6 gives a conclusion.

## 2. EVALUATED IMPAIRMENTS

There are three impairments that will be evaluated here. They are jitter, interchannel crosstalk, and GVD. Their basic knowledge is explained in section 2.1 to 2.3, respectively.

### 2.1 Jitter

Jitter is a time variation of datas bit period. It will cause the frequency variation of recovered clock signal at a receiver. Consequently, the period of data

sampling will fluctuate, possibly causing some errors in the recovered data. If the jitter becomes too severe, the clock signal may be unrecoverable by a CDR circuit and the receiver will eventually stop functioning.

The total jitter can be classified into two components [8]: Deterministic Jitter (DJ) and Random Jitter (RJ), as shown in Fig.1.

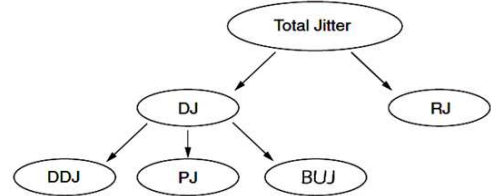


**Fig.1:** Classification of Jitter

RJ having a Gaussian histogram is always included in transmitted data. It is inherently present due to the thermal noise in electronic components as well as the shot noise from a random characteristic of arriving photons at a photodetector. Within DJ, the jitter can be further grouped as: Data Dependant Jitter (DDJ), Periodic Jitter (PJ), and Bounded Uncorrelated Jitter (BUJ). DDJ arises from the combination of Duty Cycle Distortion (DCD) and Inter-Symbol Interference (ISI). BUJ is caused by signal crosstalk. And, PJ is caused by modulation and periodic noise, such as a power supplies noise. In this paper, only PJ is investigated due to its deterministic characteristic, in addition to the inherent RJ. Since PJ can be explicitly experimented by injecting a sinusoidal wave into PG, it is commonly applied as in the cast of jitter tolerance test. In contrast, DDJ strongly depends on a chosen data pattern whereas BUJ depends on an amount of crosstalk. In this experimental setup, DDJ and BUJ are fixed due to the selected 10 Gb/s Non Return to Zero (NRZ) Pseudo Random Bit Sequence (PRBS)  $2^{31}-1$  data pattern and a constant amount of crosstalk. Hence, both DDJ and BUJ are excluded from this investigation.

Jitter can be described by the equation (1) [9], which is equivalent to phase modulation.

$$S(t) = P(2\pi f_d t + \varphi(t)) \quad (1)$$

where  $\varphi(t)$  is jitter added into the signal  $P(t)$  with  $f_d$  frequency, and  $S(t)$  is the final signal with added jitter. For example, Fig.2 shows a clock signal with added PJ. In this case, PJ is a sinusoidal wave. The period of Ideal Clock is varied by PJs amplitude, resulting in the Jittered Clock signal.

The jitter analysis requires many histograms of datas bit crossing in the eye-diagram measurement mode. As previously mention, the Gaussian histogram is a result of total RJ in a system, as shown in Fig. 3 (a). If PJ is added, the final histogram will

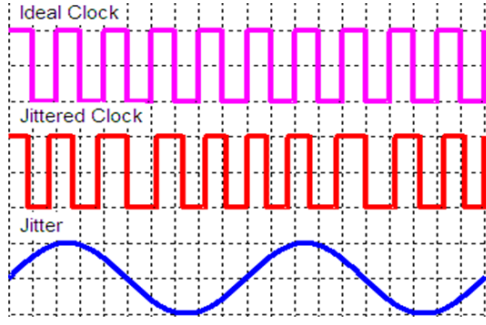


**Fig.2:** Example of Clock Signal with Periodic Jitter

become a double Gaussian shape due to the multiplication of a Gaussian histogram with a double peak histogram of PJ, as shown in Fig. 3 (b).

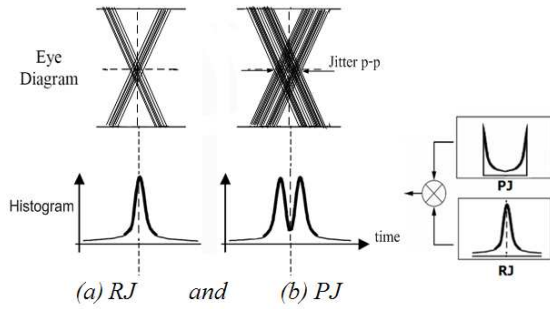


**Fig.3:** Bit Crossing of Eye-diagram and Jitter Histogram

The amount of jitter is indicated either by peak-to-peak (p-p) or root-mean-square (rms) value. p-p is the maximum jitter read at a bit crossing of eye-diagram as shown in Fig. 3, whereas rms is the average of squared jitters. The unit of jitter is in second or UI (Unit of Interval), which is the ratio of jitter in second over a bit period. The UI is preferred since it clearly indicates how severe the jitter impairment occurs within one bit period.

As described earlier, jitter will cause some errors in recovered data due to the variation in sampling period of recovered clock. The optical receiver will stop recovering data once the added jitter gets too high. This maximum amount of tolerable jitter, so called the jitter tolerance, must be measured across a frequency range. In this experiment, the PJ with a fixed frequency is injected into a system. Its amplitude is gradually increased until the systems BER reduces to a typical value of  $10^{-12}$ . This maximum amplitude of PJ is then recorded in the jitter tolerance plot, as shown in Fig. 4 [8]. Same procedures are repeated at other frequencies. The result is compared to a standard threshold line. If it lies above a threshold, the optical receiver passes standard. Otherwise, it fails if any record falls below a threshold.

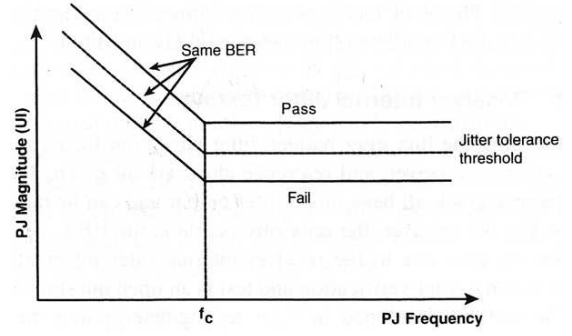


**Fig.4:** Standard Plot of Jitter Tolerance

## 2.2 Interchannel Crosstalk

The interchannel crosstalk is those unwanted power from neighbouring WDM channels that leaks into the desired channel. Thus, the interfering signals will have different wavelengths. This differs from the intrachannel crosstalk, which is more severe with interfering signals having the same wavelength as desired signal. To remove interchannel crosstalk, the optical de-multiplexer with a narrow bandpass profile and sharp wavelength cut-off is required. Any crosstalk will cause an increase in BER and power penalty. The amount of interchannel crosstalk will vary depending on the selected channel spacing. This crosstalk can be determined from the bandpass profile of optical de-multiplexer via an Optical Spectrum Analyzer (OSA). Furthermore, the crosstalk will become additional noise; resulting in the thicker lines at both data bit 1 and 0 on eye-diagram as proven later in the experimental result section. These thicker lines are clearly observed by examining the vertical histograms of bit 1 and 0 levels as well as the eye height, as shown in Fig. 5. Since the variances of both bits histograms will slightly increase, the measured eye height of recovered eye-diagram will also slightly decrease.

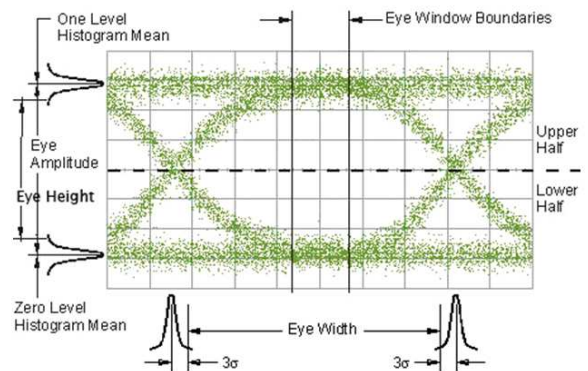


**Fig.5:** Eye-diagram with Histograms

### 2.3 Group Velocity Dispersion (GVD)

GVD is also known as the chromatic dispersion or the intramodal dispersion. It will cause pulse spreading along SMF due to the different wavelengths propagate at different speeds. GVD is a combination of material and waveguide dispersions. The variation of refractive index depending on transmitted wavelength will give rise to material dispersion; whereas the different designs of SMFs refractive index profile will control waveguide dispersion, which is always a negative value. GVD is also in effect in Multi Mode Fiber (MMF); however, the intermodal dispersion is more dominant over GVD.

Since the GVD causes pulse spreading into adjacent data bits, which is so-called Inter Symbol Interference (ISI). This increases the rise time and fall time of datas eye-diagram as well as reduces the BER performance. The rise/fall time due to GVD,  $t_{GVD}$ , can be calculated from the equation (2) [10], where  $D(\lambda)$  is the total GVD of SMF at a transmitted wavelength  $\lambda$ ,  $L$  is the total length of SMF, and  $\sigma_\lambda$  is the 3-dB spectral width of transmitted optical signal.

$$t_{GVD} \approx |D(\lambda)|L\sigma_\lambda \quad (2)$$

For SSMF, the value of  $D(\lambda)$  can be calculated from the equation (3) [10], where  $\lambda_0$  is the wavelength with zero dispersion, and  $S_0$  is the dispersion slope of total GVD at wavelength  $\lambda_0$ .

$$D(\lambda) = \frac{\lambda S_0}{4} \left[ 1 - \left( \frac{\lambda_0}{\lambda} \right)^4 \right] \quad (3)$$

Otherwise, the value of  $D(\lambda)$  between 1500 and 1620 nm wavelength can be determined from the measurement line shown in Fig. 6.  $D(\lambda)$  calculated from the equation (3) is also plotted in Fig. 6 as a dash line. The solid measurement line was exported from Agilent 860384B Photonic Dispersion and Loss Analyzer after testing the 40-km SSMF used in this

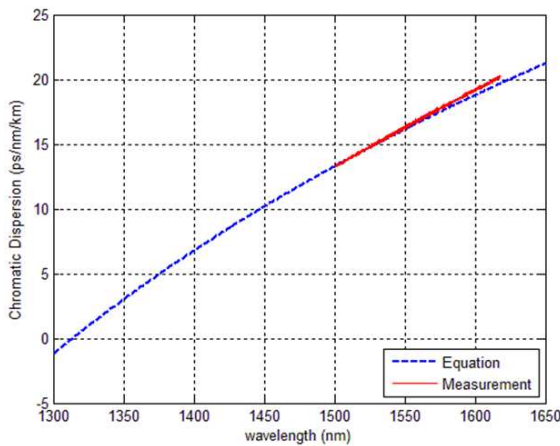


**Fig.6:** Group Velocity Dispersion versus Wavelength

experiment. According to the 40-km SSMFs datasheet from its manufacturer,  $\lambda_0$  is specified at 1313.5 nm and  $S_0$  is 0.086 ps/(nm<sup>2</sup>.km).

After calculating the rise/fall time due to GVD,  $t_{GVD}$ , from equation (2), the total rise/fall time of system,  $t_{sys}$ , can be calculated from the equation (4) [10], where  $t_{tx}$  is the rise/fall time due to an optical transmitter and  $t_{rx}$  is the rise/fall time due to an optical receiver. The total rise/fall time of system must be less than 70 percent of bit period for that transmission system to work.

$$t_{sys} = \sqrt{(t_{tx}^2 + t_{rx}^2) + t_{GVD}^2} \quad (4)$$

### 3. DESIGN OF 10 GB/S OPTICAL RECEIVER

In optical fiber communication, the optical receiver typically uses two types of semi-conductor based photodetector: Positive-Intrinsic-Negative (PIN) and Avalanche Photo-Detector (APD). PIN has lower noises and requires a lower biased voltage than APD. However, APD has a better power sensitivity and a larger output, and thus is more suitable for long distance applications. For these reasons, the APD is chosen in this design.

The 10 Gb/s optical receiver prototype consists of three main components as shown in Fig. 7: (1) APD with Trans-Impedance Amplifier (TIA) (R197AL module from Cyoptics), (2) Clock and Data Recovery (CDR) with Limiting Amplifier (LA) (MAX3991 chip from Maxim), and (3) 155.52 MHz reference clock (CCPD- 033 module from Crystek). The datasheets and schematic block diagrams of R197AL module and MAX3991 chip are available in reference [11] and [12], respectively.

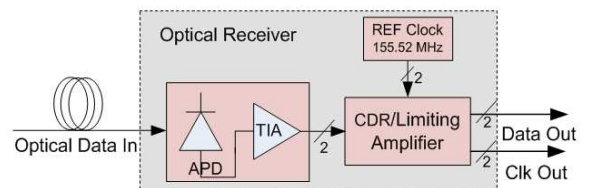


**Fig.7:** Components of 10 Gb/s Optical Receiver

All components were soldered on the 4-layered PCB as shown in Fig. 8. After 10 Gb/s NRZ optical data is launched into the optical receiver prototype via a fiber pigtail on the left of picture, APD converts this optical signal into photocurrent, and then TIA converts it into small voltage signal. Next, LA amplifies this signal up to a constant digital output and sends it through CDR. The differential 10 GHz clock output is recovered by Phase Lock Loop (PLL), whereas the differential 10 Gb/s data output is regenerated by D-Flip-Flop (DFF) inside CDR. Both data and clock outputs are CML (Common Mode Logic)



levels and have SMA connectors, located on the right and the bottom of picture. The chosen CDR requires a reference clock input at either  $1/64$  ( $=155.52$  MHz) or  $1/16$  ( $=622$  MHz) of transmitted data rate, which is exactly at 9.9532 Gb/s (STM-64).

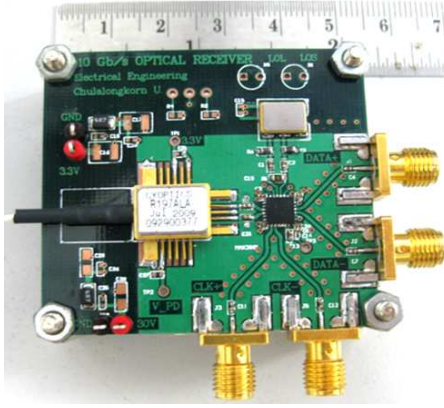


**Fig.8:** 10 Gb/s Optical Receiver Prototype

The cross-sectional view of 4-layered PCB on FR-4 dielectric is shown in Fig. 9. The signal planes are on top and bottom layers, whereas the ground and power planes are on the 2<sup>nd</sup> and 3<sup>rd</sup> layers, respectively. All dimensions are properly chosen from the cost and limitations of PCB fabrication as well as the impedance simulation results.

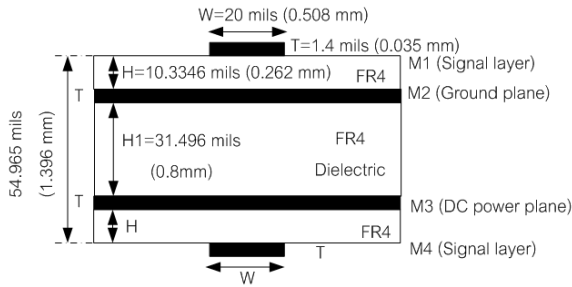


**Fig.9:** Cross-sectional View of 4-layered PCB

Since both data and clock outputs are differential signals, the differential microstrip line must be applied. Its cross-sectional view is shown in Fig. 10 (a). In some sections of signal paths, the single-ended Conductor- Backed Co-Planar Waveguide (CB-CPW) is chosen over a typical single-ended microstrip line due to its better control of the characteristic impedance, according to the simulation results given in Fig. 11. The cross-sectional view of CB-CPW is shown in Fig. 10 (b).

Several dimensions and routing of signal paths were simulated using the licensed ADS software and a free ware PolarSi8000. Their results are compared with the computation of equations in reference [13]. For example, Fig. 11 compares the impedance results of G-parameter in singled-ended CB-CPW.

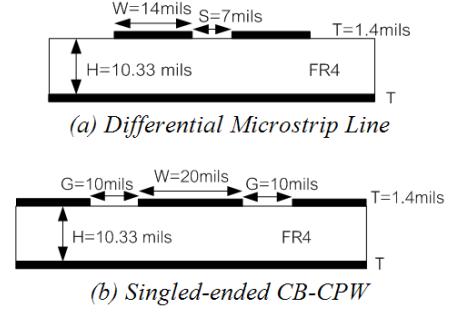


**Fig.10:** Cross-sectional Views of Signal Paths

Two versions of PCB design (straight versus curved lines) with the shortest path and the best matching impedance were fabricated.

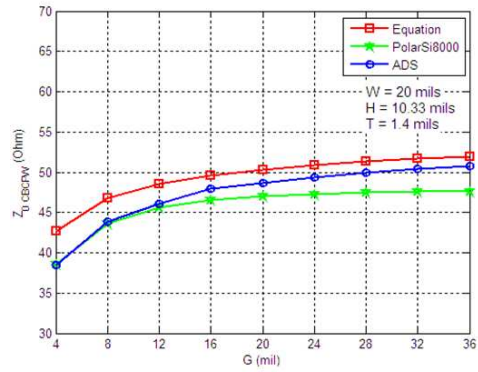


**Fig.11:** Simulation Results of CB-CPW

The measurement results of  $S_{21}$  parameters between singled-ended microstrip and CB-CPW are compared in Fig. 12. The 3-dB bandwidth of microstrip is 8.2 GHz, whereas the CB-CPWs bandwidth is beyond 10 GHz.

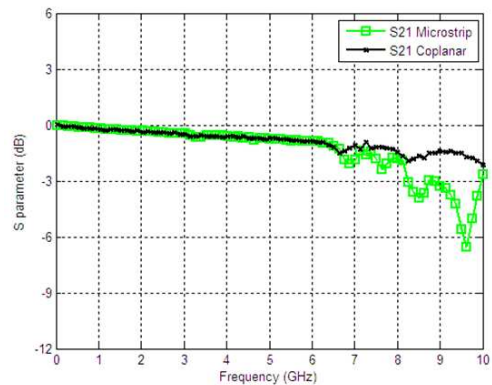


**Fig.12:** Measurement Results of  $S_{21}$  Parameter

To prove the matching impedance of designed PCB, the differential Time Domain Reflectometer (TDR) 54754A module from Agilent Technologies is connected to both data+ and data- outputs without a CDR chip, their differential impedance is measured

to be 97.67 ohms, which is almost equal to the required 100 ohms, as shown by the marker in Fig. 13.

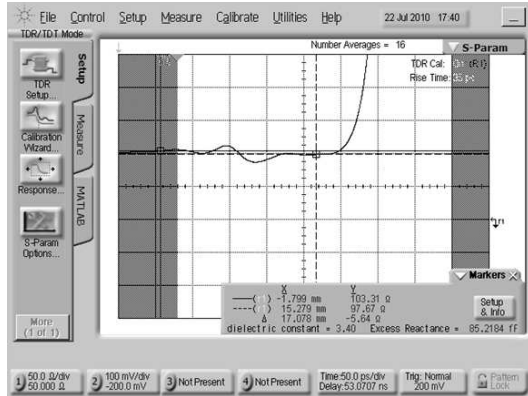


**Fig.13:** TDR Measurement of Differential Data Lines

Table 1 compares the main parameters of prototype with two commercial transceivers (from Finisar and Bookham), considering only parameters from receiver side. The prototypes bit rate can be varied by changing the reference clocks frequency, whereas the commercial transceivers do not have a fixed bit rate as they receive the reference clock from their host boards. The output level and rise/fall time are within the same ranges. This prototype can detect a wide range of wavelength and has a better sensitivity of -25.3 dBm at  $10^{-12}$  BER. Thus, it provides a larger dynamic range of (-2-(-25.3)) 23.3 dB. In addition, the maximum penalty of prototype read from BER plot is 0.8 dB (in section 5.3), which is less than that of the other two transceivers.

**Table 1:** Comparison of Receivers Parameters

Electrical Characteristics	Receiver Prototype	Finisar [14]	Bookham [15]	Unit
Data Bit Rate	9.95328	9.95-10.7	9.95-10.75	Gb/s
Different Output	575-725	340-850	360-770	mV
Data Output Rise/Fall Time	30	38	24	ps
Power Consumption	0.71 (Rx)	3.5 (Tx&Rx)	3.5 Tx&Rx)	W
<b>Optical Characteristics</b>				
Center Wavelength	1280-1610	1270-1600	1530-1560	nm
Receiver Sensitivity @ $10^{-12}$	-25.3	-24	-15.8	dBm
Receiver Overload	-2	-7	-1	dBm
Maximum Path Penalty @ 40km (20 ps/nm/km)	0.8	2 (@ 80 km)	2	dB

## 4. MEASUREMENT SETUPS

There are two main sets of measurement setups: jitter measurements and DWDM transmission testbed, as given in section 4.1 and 4.2, respectively.

### 4.1 Jitter Measurements

and jitter tolerance, as given in section 4.1.1 and 4.1.2, respectively. 10 Gb/s NRZ PRBS  $2^{31}-1$  data is generated by the BER Tester (BERT) Agilent N4901B-100 that has Pattern Generator (PG) and Error Detector (ED). The transmitter (TX) using an Electro-absorption Modulation Laser (EML) [16] sends optical data through a Variable Optical Attenuator (VOA) to simulate fiber loss. The receiver (RX) recovers 10 Gb/s data for either (1) the eyediagram measurement by DCA (Digital Communication Analyzer) Agilent 86150B 15 GHz optical / 20 GHz electrical module [17] as shown in Fig. 14, or (2) the BER measurement by ED as shown in Fig. 15. The sine wave from Signal Generator (SG) is fed to the delay input port of BERT to generate added PJ.

#### 4.1.1 Jitter Histogram from Eye-diagram

To measure jitter histogram as in Fig. 14, the DCA must be set properly to measure the histogram of datas bit crossing in eye-diagram mode. The amplitude of sine wave is set to 160 and 320 mV at two frequencies: 1 and 10 MHz. Their eye-diagrams and jitter histograms are recorded, and compared to those without added PJ. These results are analyzed in section 5.1.1.

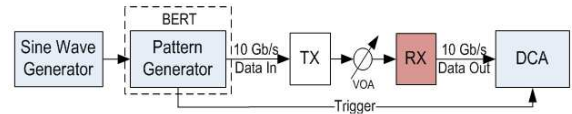


**Fig.14:** Block Diagram of Eye-diagram Measurement

#### 4.1.2 Jitter Tolerance

To measure jitter tolerance as in Fig. 15, data and clock outputs are connected to ED for BER monitoring. The sine waves frequency is fixed at one of these values: 0.7, 1, 2, 4, 10, 40 and 80 MHz. Its amplitude is gradually increased while maintaining BER better than  $10^{-12}$ . The maximum p-p jitter amplitude is recorded. The same procedures are repeated at other frequencies. The results are plotted and compared with the standard SONET/SDH threshold [18] as shown in section 5.1.2. In addition, the jitter tolerance of BERT is also measured as loop back reference by connecting PG directly to ED.

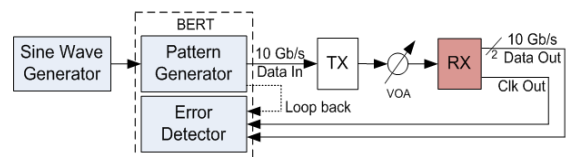


**Fig.15:** Block Diagram of Jitter Tolerance Measurement

## 4.2 DWDM Transmission Testbed

To demonstrate DWDM transmission, 3 wavelengths at 50 GHz spacing are transmitted through 40-km fiber, as described in section 4.2.1 Transmitter Side. Next, in section 4.2.2 Receiver Side, the 10 Gb/s data on center channel is dropped for eye-diagram analysis and BER measurements. The block diagram and photo of DWDM testbed are shown in Fig. 16 and 17, respectively.

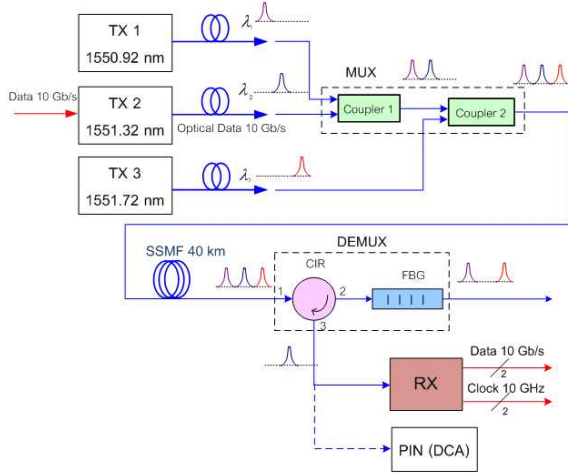


**Fig.16:** Block Diagram of DWDM Transmission

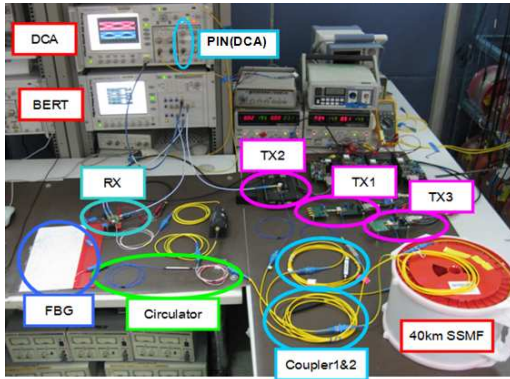


**Fig.17:** Photo of DWDM Experimental Testbed

### 4.2.1 Transmitter Side

Three transmitters (TX1, TX2 and TX3) using EML [16] have their wavelengths at 1550.92, 1551.32 and 1551.72 nm. Only the center channel is modulated with 10 Gb/s data due to a limited output from BERT, unlike in a real system where all wavelengths are modulated. However, in this case, the performance of optical receiver will not be significantly altered since these 3 wavelengths are farther apart as compared to their modulated spectra, shown later in Fig. 20. All wavelengths are multiplexed into one fiber via two 3-dB optical couplers. Their output powers after 2<sup>nd</sup> coupler are set to the same level

with a total average power of +2.2 dBm measured by an inline optical power monitor at VOA.

The fiber is a single spool of 40 km long SSF. Its total loss and length are measured by an Optical Time Domain Reflectometer (OTDR) = 7.77 dB and 39.9746 km, respectively, as shown in Fig. 18. Thus, the fiber attenuation is  $(7.77/39.9746) = 0.1944$  dB/km at ~1550 nm wavelength. Its GVD is calculated from equation (3) to be 16.21 ps/(nm.km). This GVD will increase the rise and fall times of received signal.

### 4.2.2 Receiver Side

After SSF, the center wavelength is dropped by an optical de-multiplexer, which consists of one 3-port circulator and a Fiber Bragg Grating (FBG). The transmitted and reflected profiles of FBG are measured by an Optical Spectrum Analyzer (OSA) and shown as the upper and lower lines, respectively, in Fig. 19. The transmitted profile has its bottom power level at center wavelength 30 dB below those of other wavelengths. This FBG will then reflect the center wavelength and allow two neighbouring wavelengths to propagate through. Consequently, this de-multiplexer will drop only the center wavelength for data measurement.

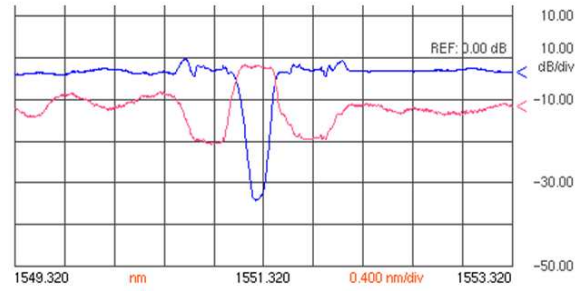


**Fig.19:** Transmitted and Reflected Profiles of FBG

In contrast, the reflected profile of FBG has its power level at center wavelength 16.9 dB higher than both sides. Therefore, the drop wavelength from de-multiplexer has its peak power 16.9 dB above those of two neighboring wavelengths, as shown in Fig. 20. This power difference indicates the amount of inter-channel crosstalk that will cause a power penalty.

After de-multiplexer, 10 Gb/s data is recovered by the receiver prototype. However, its output level does not vary proportionally with input power due to the data regeneration inside CDR circuit. As a result, the effects of both crosstalk and GVD cannot be clearly observed from the recovered eye-diagrams. For this particular reason, the PIN receiver Agilent 86105B module inside DCA, which has a linear characteristic detection, is temporary used instead for the observation of worsen eye-diagrams, but never for the performance comparison with receiver prototype. The photo of PIN receiver is shown in Fig. 21. This PIN receiver has degraded over the years. Its current sen-

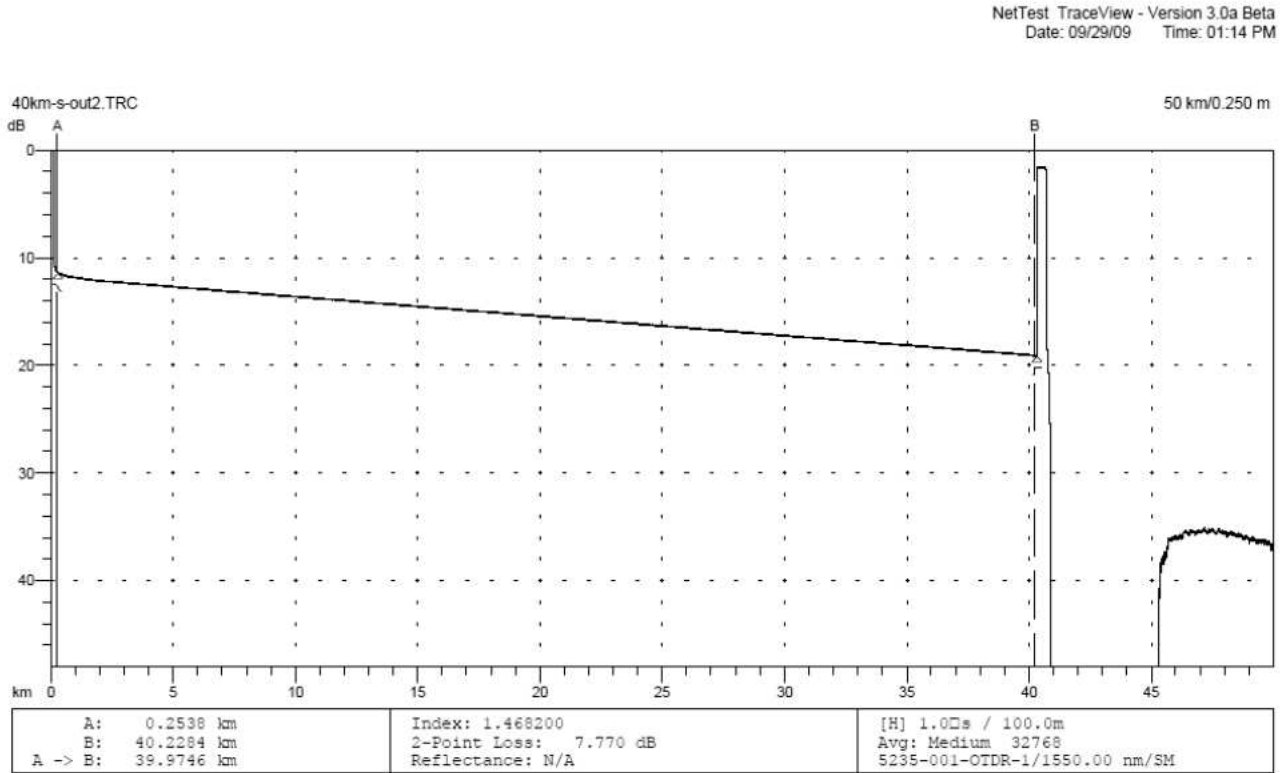


**Fig.18:** OTDR Measurement of 40-km SSMF

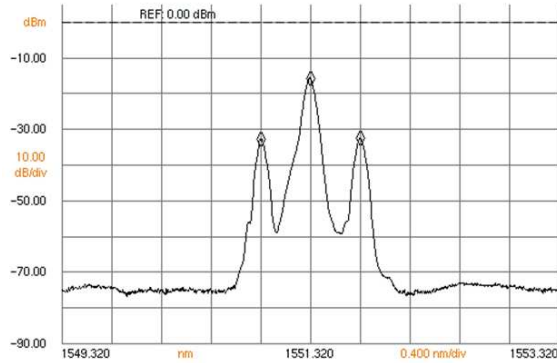


**Fig.20:** Spectrum of Received Optical Signal



**Fig.21:** PIN Receiver inside DCA

sitivity is relatively worst at -6.3 dBm for  $10^{-9}$  BER. Hence, its input power must be above that level for the PIN receiver to functionally perform optical-to-electrical data conversion.

## 5. EXPERIMENTAL RESULTS

There are three main sets of experimental results: (1) jitter, (2) crosstalk and dispersion, and (3) BER, as described in section 5.1, 5.2 and 5.3, respectively.

### 5.1 Jitter Results

Two jitter results are jitter histograms of added PJ, and jitter tolerance of receiver prototype, as de-

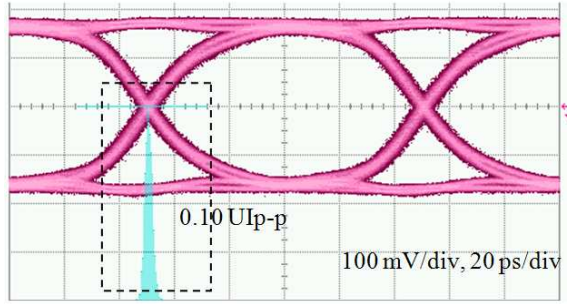
scribed in section 5.1.1 and 5.1.2, respectively.

#### 5.1.1 Jitter Histogram Results

Fig. 22 shows the recovered 10 Gb/s eye-diagram from receiver prototype before adding PJ. The resulted jitter histogram inside a dash rectangle has only one Gaussian profile due to inherent RJ in this transmission system. This shape is in agreement with Fig. 3(a). The measured total p-p jitter and rms jitter are  $0.1 \text{ UI}_{\text{p-p}}$  and  $0.013 \text{ UI}_{\text{RMS}}$ , respectively.

After adding PJ, at two different amplitudes and frequencies of sine wave, the resulted jitter histograms are compared in Table 2. Obviously, the jitter histograms become double Gaussian peaks due to a combination of system RJ and added PJ. These results

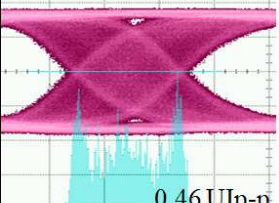
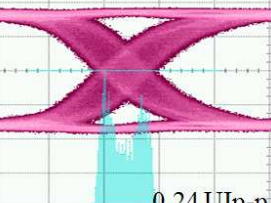
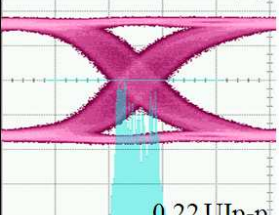
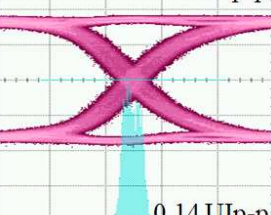




**Fig.22:** 10 Gb/s Eye-diagram with Jitter Histogram Before Adding Periodic Jitter

are in agreement with Fig. 3 (b). The total p-p jitters are also measured and reported in Table 2. The analysis of these p-p jitters indicates that the total jitter will be proportional to the applied amplitude of sine wave, which in agreement with equation (1). However, it will be inversely proportional to the applied frequency of sine wave. Due to the jitter transfer characteristic of chosen CDR chip, the measured total jitter will be reduced at those applied frequencies above 1 MHz.

**Table 2:** Jitter Histograms when the Voltage and Frequency of Input Sine Wave is Varied

	$f = 1 \text{ MHz}$	$f = 10 \text{ MHz}$
$V = 320 \text{ mV}$	 0.46 UIp-p	 0.24 UIp-p
$V = 160 \text{ mV}$	 0.22 UIp-p	 0.14 UIp-p

### 5.1.2 Jitter Tolerance Results

Fig. 23 shows the measured jitter tolerances at 10-12 BER of optical receiver prototype, RX line, and BERT, Loop back line. Since the RX line is above the SONET standard [18], SONET MASK line and is below the Loop back' line as expected, this receiver passes the standard jitter tolerance test. The explanation for higher tolerance at lower frequency is due to a slow change in phase such that the clock recovery circuit can rapidly complete its phase locking.

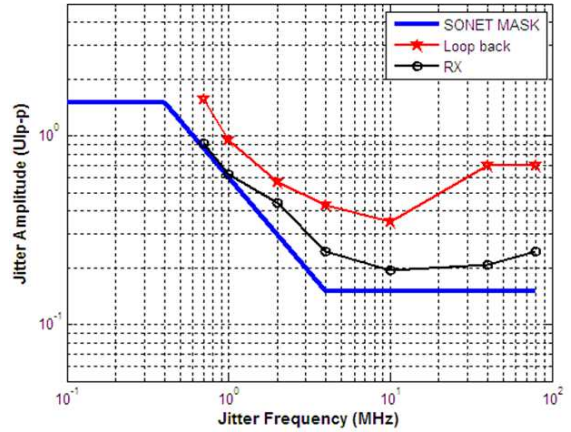


**Fig.23:** Comparison of Measured Jitter Tolerances

## 5.2 Crosstalk and Dispersion Results

The effects of interchannel crosstalk and GVD on eye-diagrams detected by PIN receiver and recovered by receiver prototype are described in section 5.2.1 and 5.2.2, respectively.

### 5.2.1 Eye-diagram from PIN receiver inside DCA

1) *Crosstalk Effect:* The transmission testbed is set as in Fig. 16, but without 40-km SSF. The detected 10 Gb/s eye-diagram from PIN receiver with one wavelength and three wavelengths transmitted at the same average input power of -6 dBm are shown in Fig. 24(a) and Fig. 24(b), respectively.

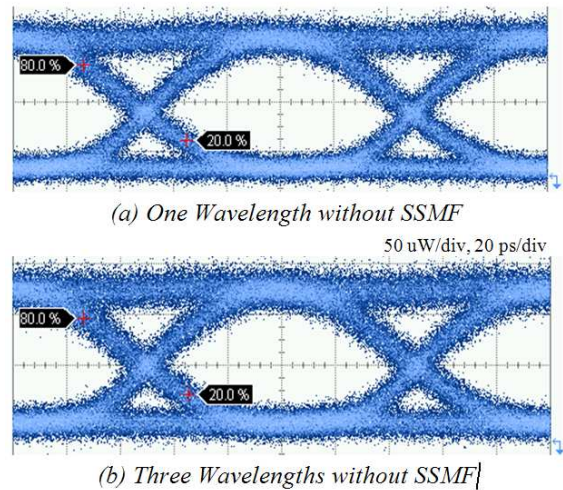


**Fig.24:** PINs Eye-diagrams with 1 & 3  $\lambda$ s

After a careful examination of the line thickness of bit 1 and 0 on eye-diagrams in Fig. 24, the crosstalk effect is very slightly shown as a thicker line in Fig. 24(b). This little difference is due to the very low interchannel crosstalk level of 16.9 dB from FBG.

2) *GVD Effect:* The testbed is set as in Fig.16, with only the center wavelength transmitted and thus without a de-multiplexer due to its insertion loss. The

eye-diagrams of one wavelength without fiber and with 40-km SSMF are shown in Fig. 25(a) and Fig. 25(b), respectively.

Comparing the two eye-diagrams in Fig. 25, they clearly show an increase in the rise and fall times due to GVD impairment. The measured rise and fall times in Fig. 25(a) are 23.6 and 25.8 ps, respectively; whereas the rise and fall times in Fig. 25(b) are 53.8 and 54.2 ps, respectively. From these results, the GVD effect of 40-km SSMF can be analyzed as follows.

First, the GVD is calculated from equation (3) to be 16.21 ps/(nm.km). Then, the rise/fall time due to GVD is calculated from equation (2):  $t_{GVD} = 16.21 \times 40 \times 0.06 = 38.904$  ps. The measured rise and fall times in Fig. 25(a) are the combined rise/fall time from transmitter and receiver, without GVD, as given in equation (4). Hence, the total rise and fall times of entire transmission system are recalculated from equation (4), using the calculated  $t_{GVD}$  together with the measured rise and fall times in Fig. 25(a), = 45.50 and 46.68 ps, respectively. These numbers are slightly lower than the measured results at 53.8 and 54.2 ps, probably due to the inaccurate measurement of very distorted and noisy eye-diagram in Fig. 25(b).

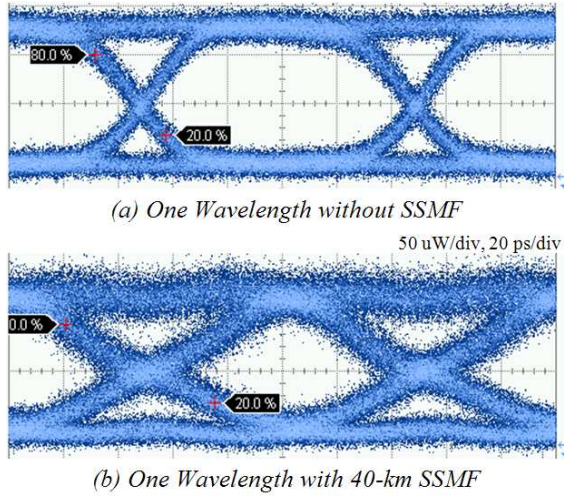


**Fig.25:** PINs Eye-diagrams with  $\mathcal{E}$  without SSMF

### 5.2.2 Eye-diagram from Optical Receiver Prototype

1) *Crosstalk Effect*: The testbed is set as in Fig. 16, without 40-km SSMF. The recovered 10 Gb/s eyediagram by receiver prototype with one wavelength and three wavelengths transmitted at the same average input power of -26 dBm are shown in Fig. 26(a) and Fig. 26(b), respectively.

A careful comparison between two eye-diagrams in Fig. 26 concludes that the crosstalk effect is unnoticeable due to the data regeneration of prototype. In the middle of eye-diagram, the bit 1 and 0 outputs are always fixed to the CML level, as described in section 3. Hence, this receiver can reduce the crosstalk

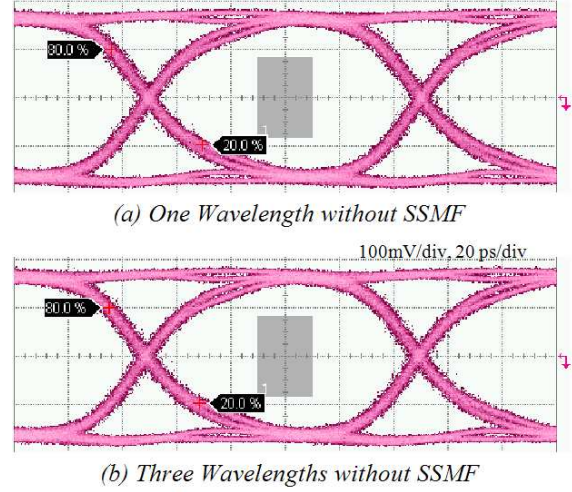


**Fig.26:** Prototypes Eye-diagrams with  $1\mathcal{E}$  3  $\lambda$ s

impairment.

2) *GVD Effect*: The testbed is set as in Fig.16, with three wavelengths transmitted. The eye-diagrams of three wavelengths without fiber and with 40-km SSMF at the same averaged power of -26 dBm are shown in Fig. 27(a) and Fig. 27(b), respectively.

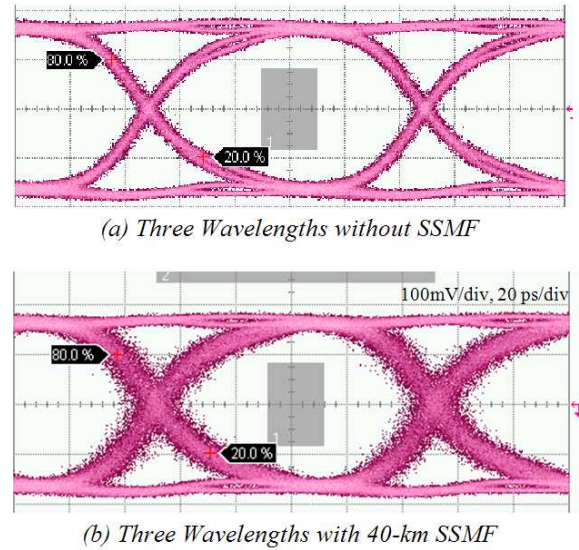


**Fig.27:** Prototypes Eye-diagrams with  $\mathcal{E}$  without SSMF

Comparing these two eye-diagrams in Fig. 27, they clearly show a broad and noisy spread of bit crossing due to GVD impairment. In the middle of eye-diagram, the bit 1 and 0 outputs are again fixed to the same CML levels. The measured rise and fall times are 31.6 and 33.3 ps, respectively. These numbers are much less than those from PIN receiver in Fig. 25 (b) due to data regeneration. For that reason, this receiver can significantly reduce the GVD impairment. The eye-diagram in Fig. 27 (b) also passes the standard STM-64/OC-192 data mask, shown as



a gray rectangle at center as well as the upper and lower borders.

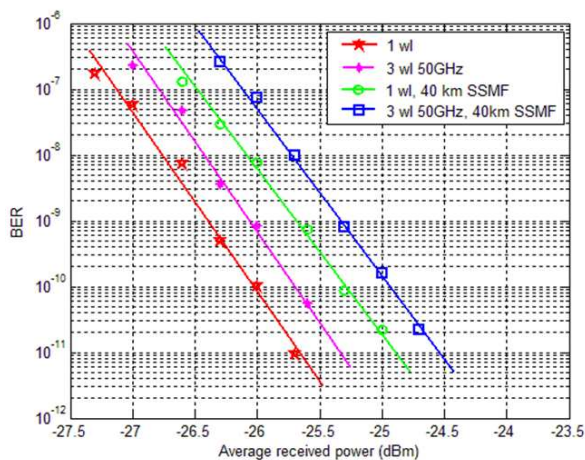
### 5.3 Bit Error Rate Results

Fig. 28 shows the BER performance of 10 Gb/s optical receiver prototype under four transmission cases: (1) only the center wavelength transmitted (*1wl*), (2) three wavelengths transmitted at 50 GHz spacing (*3wl50GHz*), (3) the center wavelength transmitted over 40-km SSMF (*1wl+40kmSSMF*), and (4) three wavelengths transmitted at 50 GHz spacing over 40-km SSMF (*3wl50GHz + 40kmSSMF*). Evidently, the BER results will shift upward as the interchannel crosstalk and GVD effects are included in the experimental transmissions.

In order to determine the power penalty or path penalty of this prototype, first, the average received optical powers at  $10^{-9}$  BER must be read from Fig. 27. According to those four transmission cases, their corresponding received powers are -26.4, -26.1, -25.7 and -25.3 dBm, respectively. Subsequently, the penalty is calculated as a power difference between a pair of those numbers, as follows.

1) *Crosstalk Effect*: The penalty between 3wl 50GHz case and 1wl case is  $(-26.1 - (-26.4)) = 0.3$  dB, whereas the penalty between 3wl 50GHz+40km SSMF case and 1wl+40km SSMF case is  $(-25.3 - (-25.7)) = 0.4$  dB. These two power penalties arise from the interchannel crosstalk impairment.

2) *GVD Effect*: Similarly, the penalty between 1wl+40km SSMF case and 1wl case is  $(-25.7 - (-26.4)) = 0.7$  dB, whereas the penalty between 3wl50GHz + 40kmSSMF case and 3wl case is  $(-25.3 - (-26.1)) = 0.8$  dB. These two penalties arise from the GVD impairment. They both are lower than the 2 dB maximum penalty specified in the G.691 standard [7].



**Fig.28:** BER Plot of 10 Gb/s Optical Receiver Prototype

## 6. CONCLUSION

The design of 10 Gb/s optical receiver prototype using an APD with integrated TIA, a CDR chip with LA, and a 155.52 MHz reference clock is described. All components are successfully integrated onto the 4-layered FR-4 PCB. The two selected types of signal paths are differential microstrip line and single-ended CB-CPW. Their dimensions are optimally chosen for the lowest cost and matching impedance, according to the equations and the simulations from ADS and PolarSi8000 software. The prototypes performance has been evaluated under three impairments: jitter, inter-channel crosstalk and GVD. The double Gaussian histograms of added PJ are analyzed to be proportional to amplitude and inversely proportional to frequency of applied sine wave. The jitter tolerance of prototype passes the SONET threshold with BER below  $10^{-12}$ . The experimental testbed of three 50-GHz DWDM wavelengths transmitted over 40 km long SSMF is demonstrated. The effects of crosstalk and GVD on eyediagrams are observed as the slightly thicker bit levels and the increase in rise and fall times, respectively. The measured rise and fall times are analyzed under GVD effect. The recovered eye-diagrams from prototype show that its design can reduce both crosstalk and dispersion effects. The BER performance of prototype are reported under four transmission cases, and the power penalty at 100mV/div, 20 ps/div  $10^{-9}$  BER is determined to be 0.8 dB due to GVD effect. This value is within the standard limit of 2 dB.

## 7. ACKNOWLEDGEMENT

This research was supported by Telecommunications Research and Industrial Development Institute (TRIDI), the National Telecommunications Commission (NTC). In addition, T&M equipment is supported by Cooperation Project between Department of Electrical Engineering and Private Sector for R&D, Chulalongkorn University, and the Excellence Group of Chulalongkorn University in Lightwave and High-Speed Communications, sponsored by TRIDI, the NTC.

## References

- [1] Y. Amamiya, S. Kaeriyama, H. Noguchi, Z. Yamazaki, T. Yamase, K. Hosoya, M. Okamoto, S. Tomari, H. Yamaguchi, H. Shoda, H. Ikeda, S. Tanaka, T. Takahashi, R. Ohhira, A. Noda, K. Hijioka, A. Tanabe, S. Fujita, N. Kawahara "A 40Gb/s Multi-Data-Rate CMOS Transceiver Chipset with SFI-5 Interface for Optical Transmission Systems," *The 2009 IEEE International Solid-State Circuits Conference*, pp. 358-359, February 2009.
- [2] H-G. Yun, K-S. Choi, Y-H. Kwon, J-S Choe, and JT. Moon, "Fabrication and Characteristics

- of 40 Gb/s Traveling-Wave Electroabsorption Modulator- Integrated DFB Laser Modules," *The 2006 Electronic Components and Technology Conference*, 2006.
- [3] T. Sakamoto, S. Nobuo, S. Koike, K. Hadama, and K. Naoya, "4 channel  $\times$  10 Gbit/s Optical Module for CWDM Links," *The 2004 Electronic Components and Technology Conference*, vol. 1, pp. 1024-1028, 2006.
- [4] A. Narasimha, B. Analui, Y. Liang, T.J. Sleboda, S. Abdalla, E. Balmater, S. Gloeckner, D. Guckenberger, M. Harrison, R.G.M.P. Koumans, D. Kucharski, A. Mekis, S. Mirsaidi, Dan Song, T. Pinguet, "A Fully Integrated 4  $\times$  10-Gb/s DWDM Optoelectronic Transceiver Implemented in a Standard 0.13  $\mu$ m CMOS SOI Technology," *IEEE Journal of Solid-State Circuits*, Vol. 42, No. 12, December 2007
- [5] H. H. Lee, J. M. Oh, D. Lee, G. W. Lee, and S. T. Hwang, "Performance of 16 $\times$ 10 Gb/s WDM Transmissions Over 4 $\times$ 40 km of SMF Using Linear Optical Amplifier Combined With Raman-Pumped Dispersion Compensation Fiber Under Dynamic Add-Drop Situations," *IEEE Photonic Technology letter*, Vol.16, No.6, pp. 1576-1578, 2004.
- [6] Dayou Qian, Jianjun Yu, Ting Wang, "Ultra-highcapacity optical transmissions," *Communications and Photonics Conference and Exhibition (ACP)*, Shanghai, China, 2-6 Nov. 2009
- [7] "ITU-T G.691: standard of optical interfaces for single channel STM-64 and other SDH systems with optical amplifiers," [www.itu.int](http://www.itu.int)
- [8] M. P. Li, Jitter, *Noise and Signal Integrity at High-Speed*, Pearson Education, 2008.
- [9] Agilent Technology, "Jitter Analysis Techniques for High Data Rate," Application Note 1432, 2003.
- [10] G. Keiser, *Optical Fiber Communications*, 3<sup>rd</sup> edition, McGraw-Hill, 2000.
- [11] CyOptics, Inc., "R197AL 10 Gb/s Small Form-Factor Co-Planar APD-TIA Receiver with Linear TIA for EDC Applications," [www.cyoptycs.com](http://www.cyoptycs.com)
- [12] Maxim Integrated Products, "MAX3991 10 Gbps Clock and Data Recovery with Limiting Amplifier," [www.maxim-ic.com](http://www.maxim-ic.com)
- [13] K.C. Gupta, R. Garg, I. Bahl, P. Bhartia, *Microstrip Lines and Slotlines*, Artech House, 1996.
- [14] Finisar Corporation, "10 Gb/s 80 km XFP Optical Transceiver, FTRX-1811-3," [www.finisar.com](http://www.finisar.com).
- [15] Bookham Technology, "IGF32511,XFP Optical Transceiver for 40 km 10 G Serial applications," [www.bookham.com](http://www.bookham.com).
- [16] Palatorn Sricham, Pattarakamon Rangsee and Duang-rudee Worasuchee, "A 2.5 Gb/s Electro-Absorption Modulator Integrated Laser Optical Transmitter in Long-Haul Dense Wavelength Division Multiplexing Transmission," *Proceeding of 2010 ECTI International Conference on Electrical Engineering/Electronics, Computer, Telecommunications and Information Technology*, vol. 1, pp. 253-256, 2008.
- [17] Agilent Technologies, "Infiniium DCA-J Agilent 86100C Wide-Bandwidth Oscilloscope Mainframe and Modules," 5989-0278EN, [www.agilent.com](http://www.agilent.com).
- [18] "SONET/SDH specifications" are ITU-T0.172 from [www.itu.int](http://www.itu.int) and GR-253-CORE from [www.telcordia.com](http://www.telcordia.com).



**Duang-rudee Worasuchee** received dual B.S. degrees in Engineering Physics and Electrical Engineering from Lehigh University, Pennsylvania, U.S.A. in 1995. She received the M.S. and Ph.D. degrees in Electrical Engineering from Stanford University, California, U.S.A. in 1997 and 2002. Since 2002, she joined the Department of Electrical Engineering, Chulalongkorn University, Bangkok, Thailand, as a lecturer and currently she is an Assistant Professor. Her research activities are in Optical Fiber Communications and Networks, High-speed Optical Transceiver and Digital Signal Integrity.



**Wanee Srisuwarat** was born in Chonburi, Thailand, on February 19, 1986. She received the B.Eng. and the M.Eng degree in Electrical Engineering from Chulalongkorn University, Bangkok, Thailand, in 2007 and 2009, respectively. Her research topic has involved with a development of 10 Gb/s Optical Receiver Prototype using an Avalanche Photo-Detector.



**Jirawut Akaranuchat** was born in Sukhothai, Thailand, on September 9, 1986. He received the B.Eng. degree in Electrical Engineering from Chulalongkorn University, Bangkok, Thailand, in 2008. He is currently working toward the M.Eng. degree in Electrical Engineering at Chulalongkorn University, Bangkok, Thailand. His current research topic is related to the design of 10 Gb/s Optical Transmitter Prototype

with Temperature Control System using PID control circuit.